Available online at www.sciencedirect.com
ScienceDirect
Journal of the European Ceramic Society 28 (2008) 3049–3057
www.elsevier.com/locate/jeurceramsoc

Defect and microstructural evolution during drying of soapnut-based alumina foams

Mamata Pradhan [a,1], Parag Bhargava [b,*]

[a] *Materials Science Centre, IIT Kharagpur, Kharagpur, West Bengal 721302, India*
[b] *Metallurgical Engineering & Materials Science, IIT Bombay, Powai, Mumbai 400076, India*

Received 15 November 2007; received in revised form 25 April 2008; accepted 2 May 2008
Available online 14 July 2008

Abstract

The present study demonstrates the use of soapnut, a naturally occurring surfactant for producing alumina ceramic foams. A range of slurry compositions with soapnut amounts ranging from 2 to 20 wt% in water, alumina loading of 35–55 vol% were studied. Though all slurry compositions foamed when subjected to mechanical agitation the formation of green ceramic foams free of macroscopic defects was found to be strongly dependent on conditions during drying of foamed slurries. Addition of guar gum to the slurries was shown to enhance foam stability and thus produce defect-free foams from compositions that otherwise either collapsed or resulted in other macroscopic defects during drying. Drying conditions also had a strong effect on microstructural parameters such as cell size and cell connectivity. Soapnut-based foams appear to have a greater connectivity between cells than foams produced by other comparable processes.

Keywords: Al_2O_3; Soapnut; Foam stability; Drying; Defects; Cell size gradient; Cell connectivity

1. Introduction

Ceramic foams are known to possess high chemical inertness, high temperature and thermal shock resistance, high specific strength, low thermal mass and low thermal conductivity.[1–6] Owing to these properties ceramic foams are used in applications such as in kiln furniture, porous burners, air heating systems, gas turbine combustion chambers, steam generators, catalyst carriers, molten metal and hot gas filters.[2–6] Ceramic foams are also proposed for use in biomedical implantation and sensors.[6,7] Ceramic foams can be fabricated by a number of methods such as infiltration of ceramic slurry to synthetic and natural preforms, incorporation of fugitives to ceramic slurry, direct foaming of mixture of polyurethane precursor with ceramic powder, direct foaming of slurry with use of surfactants, etc., each of which yield different microstructures.[7–57] Among the methods mentioned above direct foaming is one of the most versatile in terms of controlling porosity, microstructure, and overall the process is cost effective. In direct foaming process, major microstructural changes occur during consolidation of foamed slurry either by drying, gelling or freezing.[40–58] Foams processed by direct foaming of slurries have a tendency to develop defects such as cracks, delamination, warpage during drying. The capillary stress rise due to evaporation of water from the surface plays a role in formation of cracks.[59,60] The present study describes use of soapnut as a natural surfactant cum binder in making ceramic foams and is mainly focused on the influence of composition and drying conditions on sintered microstructure and defects in ceramic foams.

2. Experimental procedure

2.1. Characterization of soapnut extract

Soapnut fruit belongs to the genus of *Sapindus* in the Sapindaceae family and the one that was used in the present study possesses the botanical name *Sapindus mukorossi* popularly known as Reetha in India. The water-soluble extract from *S. mukorossi* was used in the preparation of ceramic foams. The soapnut extraction procedure has been described in detail

* Corresponding author. Tel.: +91 22 25767628; fax: +91 22 25723480.
E-mail address: pbhargava@iitb.ac.in (P. Bhargava).
[1] Presently in Tata Research Development and Design Centre, Tata Consultancy Services, 54B, Hadapsar Industrial Estate, Hadapsar, Pune 411013, India.

0955-2219/$ – see front matter © 2008 Elsevier Ltd. All rights reserved.
doi:10.1016/j.jeurceramsoc.2008.05.025

elsewhere by the same author.[58] The as-extracted soapnut solution is acidic and has a pH of around 5. For any possible variations in concentration, the extracted soapnut solutions prepared from different batches of the soapnut fruit were examined using UV–vis spectroscopy (Spectrascan UV 2600 digital spectrophotometer, Chemito, India).

Diluted soapnut solution (0.05 wt%) with concentrated sulphuric acid (98.8 wt%) forms reddish pink color, which shows an absorbance peak at 524 nm[61,62] due to the presence of terpene ring in saponin. This absorbance peak was utilized for precise determination of concentration of soapnut solutions. The dried powder of the water-soluble soapnut components was used to prepare solutions of different known concentrations. A calibration curve was obtained from the absorbance values of five different known concentrations at 524 nm. The concentration of the freshly prepared soapnut extract solutions was calculated from the calibration curve.

The functional groups present in the extract were characterized by Fourier Transform Infrared spectroscopy (FTIR). Single beam spectra of aqueous soapnut extract in a KBr matrix were obtained in the frequency range (4000–500 cm^{-1}) and were referenced against KBr background (Nexus 870, Thermo Nicolet, Madison, WI, USA). Molecular weight or average molecular weight of soapnut extract was calculated using double beam differential refractometer (DRM-1021, Photal, OTSUKA electronics) and super dynamic light scattering spectrophotometer (DLS-7000, Photal, OTSUKA electronics). Presence of inorganic residue such as sodium, potassium, and calcium in soapnut extract was analyzed by flame photometer (Model No. CL378, Elico Limited). Photometry of the soapnut extract indicated the presence of less than 1 wt% of inorganic impurities with significant ones being 90 ppm of Na, 260 ppm K and 160 ppm Ca.

2.2. Slurry preparation and foaming

The different alumina slurry compositions prepared using freshly extracted soapnut are shown in Table 1. The slurry compositions have been represented as (x, y) in all discussions in the text where x represents the alumina particle loading and y represents the concentration of soapnut in water.

On the basis of preliminary observations, for all foaming experiments 60 ml of slurry was taken with 100 gms of zirconia media (2–3 mm diameter) in a 300-ml polypropylene container and the foaming was carried out by tumbling the container for 3 h. Details of the procedures for slurry preparation, foaming, rheological characteristics of the slurries were described earlier.[58]

2.3. Casting and setting of ceramic foams

The foamed slurries were cast into Vaseline-coated Perspex molds with dimensions of 93 mm × 50 mm × 13 mm. Ceramic foams were dried and set at different temperatures in a preheated oven. The binder burn out of the green foamed samples was carried out in accordance with results of thermogravimetric analysis. Thermogravimetric analysis (TGA) of the ground soapnut powder and green ceramic foam produced from soapnut-based slurries were carried out up to 900 °C in air at a heating rate of 10 °C/min (Diamond DT-TGA, PerkinElmer, USA). All samples were sintered at 1600 °C for 2 h.

2.4. Characterization of sintered foams

All sintered ceramic foam samples were characterized for percent open, closed and total porosity by Archimedes principle using water as the immersing medium (ASTM C 693, C20-00). As sawed sections of the foam samples were characterized using stereomicroscope (SZ 1145 TR PT, Olympus Model, Japan) and scanning electron microscope (SEM, JSM 5800, JEOL, Japan). The sawed surface of alumina foam was coated with ink to enhance the contrast when viewing under stereomicroscope. SEM micrographs of the ceramic foams were characterized using image analysis software (Image Tool, Version 3.0, University of Texas Health Science Center, San Antonio).

Table 1
Slurry compositions, viscosity, extent of foaming and porosity of resulting foams

Experiment number	Solids loading (vol%)	Soapnut amount (wt%)	Viscosity (Pa s) at shear rate (10 s^{-1})	Extent of foaming	Porosity (%)
1		20	11	1.6	61.4
2		15	9.5	1.9	67.4
3	55	10	5.5	2.3	70.5
4		5	2.8	2.7	76.4
5		2	2.7	3.1	78.5
6		20	3.5	3.1	81.5
7		15	2.8	3.5	83.6
8	45	10	1.4	5.5	85.3
9		5	0.5	5.5	86.6
10		2	0.4	5.5	88.4
11		20	1.3	4.7	86.4
12		15	0.6	5.5	89.3
13	35	10	0.5	5.5	90.6
14		5	0.1	5.5	90.9
15		2	Too fluid	5.5	Not stable

3. Results and discussion

3.1. Characteristics of soapnut extract and slurry

Consistency in concentration of soapnut solutions prepared from the fruit pericarp was checked by monitoring solutions from several batches at random. Results of UV–vis spectroscopy of the freshly prepared extracts confirmed that there was negligible measurable variation (±0.05 wt.%) in the concentration even when it was prepared from different batches of the fruit.

It is well documented in the research literature [63–65] that the presence of saponin in aqueous soapnut extract is largely responsible for the significant lowering of the surface tension. Soapnut is an excellent surfactant as was evident from the lowering of surface tension [63–65] of water from 72 to 40 mN/m upon addition of soapnut to water. Experiments with aqueous foams devoid of particles also illustrated the capability of soapnut in stabilizing foams. The rate of solvent drainage from aqueous foams reduced from 150 to 115 μl/s upon increasing the concentration of soapnut from 2 to 5 wt%.

The presence of various functional groups forming hydrophobic and hydrophilic part of soapnut which contribute to it becoming an effective foam stabilizer [55,56] were confirmed through FTIR. The presence of hydroxyl groups was indicated by the absorbance peak at 3446 cm^{-1} in FTIR spectra (Fig. 1). FTIR spectra of soapnut also showed absorbance peaks at 1635 and 1049 cm^{-1} suggesting the presence of acids, carbohydrates, respectively. The carbohydrates ascribed to gums in the soapnut[66] were expected to provide binding action for ceramic particles. The binding ability of the soapnut constituents could also be linked to their relatively high average molecular weight, which was measured by dynamic laser scattering experiments to be around 10^5 Da.

The non-ionic nature of soapnut is an advantage as its presence does not result in changes in ionic strength thus may not affect stabilization of ceramic particles in slurries.[67] Soapnut

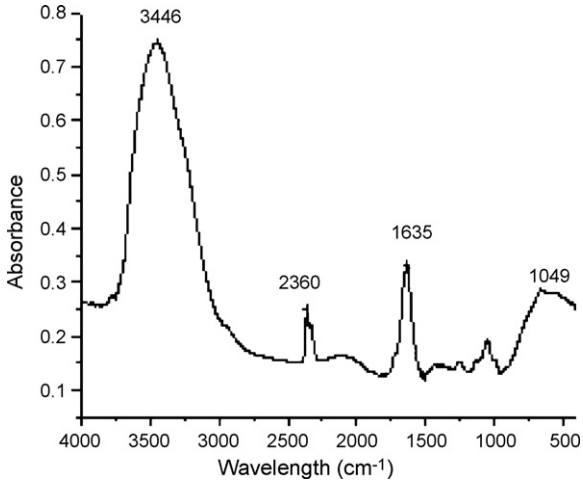

Fig. 1. FTIR spectrum of the soapnut extract.

premix of different concentrations were used in making alumina slurries. The spectrum of slurry compositions with different combinations of ceramic loading and soapnut concentration in water (Table 1) spanned a wide viscosity range (0.1–11 Pa s) measured at shear rate of 10 s^{-1}. Viscosity played a deterministic role in foaming behaviour of the slurries [52,53,55–58] as has been discussed in a prior publication.

3.2. Defect evolution in green ceramic foams

The foamed slurries were cast into perspex molds and subjected to drying at different temperatures (Table 2). The observations regarding drying of foam samples described below must be viewed in light of the fact that the foamed slurries were cast in rectangular molds with the top open. Thus, the drying of foams had to occur only from the top surface.

Drying the foams both at slow and fast rates resulted in macroscopic defects (Fig. 2). When the foams were dried slowly at

Table 2
Influence of drying temperature on setting of foams made from slurries with different compositions

Number	Ceramic loading (vol%)	Slurry composition		Extent of foaming	Status of sample: longitudinal crack (LC), collapse and width wise crack (CL), defect free (F), delamination (D)			
		Soapnut amount (%) in premix	Soapnut amount (%) with respect to powder weight		30 °C	40 °C	50 °C	60 °C
1	55	20	3.9	1.6	F	F		
2		15	2.9	1.9	F	F		
3		10	1.9	2.3	F	F		
4		5	0.98	2.7	F	F		
5		2	0.39	3.1	F	F		
6	45	20	6	3.1	–	F	F	F
7		15	4.5	3.5	–	F	F	F
8		10	3.0	5.5	–	F	F	F
9		5	1.5	5.5	CL	D	D	D
10		2	0.6	5.5	CL	CL (partial)	D	LC[a]
11	35	20	9.2	4.7	CL	CL	F	F
12		15	6.9	5.5	CL	CL	F	F
13		10	4.6	5.5	CL	D	LC[a]	LC[a]
14		5	2.3	5.5	CL	D	LC[a]	LC[a]

[a] All LC visible within 1 h after drying is initiated.

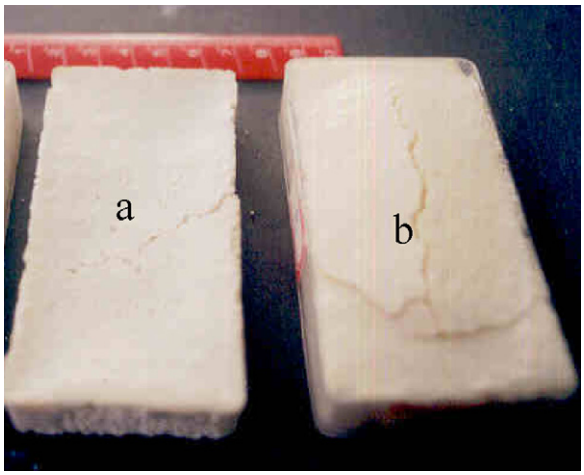

Fig. 2. Dried foams showing (a) crack along the width accompanying foam collapse and (b) longitudinal crack due to expansion of bubbles.

ambient temperature of around 30 °C, the foams prepared from (35, 5) and (35, 10) slurries collapsed, accompanied by the formation of cracks across the sample width (Fig. 3a). The collapse of foams was a result of the long drying period exceeding 24 h over which the drainage of solvent occurred before the drying and setting of the foam structure could be completed. It is notable that when the same foam samples were dried at higher temperature of 40 °C the foams did not collapse but the samples developed delamination cracks (Fig. 3b). These observations hinted to the fact that drying at 40 °C though was fast enough to prevent collapse but was not able to prevent the effects due to differential drying from top to bottom. Visual observation also suggested that during drying at 40 °C, while the top layer dried and became firm the bottom layer was still undergoing drying. Due to the delayed drying when the bottom layer shrunk, it caused a separation from the already firmed up top layer resulting in delamination type of cracks.

Raising the drying temperature to 50 °C though eliminated the problem of delamination but caused development of a new type of defect—longitudinal cracks, which appeared within an hour after the samples were kept for drying in a preheated oven. The foam samples appeared to have expanded in volume (Figs. 2b and 3c.) projecting out of the mold cavity and only one major crack developed along the length of the samples. The above observations indicate that the heat conducted through the bottom of the mold that was resting on the stainless steel (SS) shelves inside the oven caused expansion of air in the bubbles which led to the observed cracking. The cracking as observed above was encouraged by the existence of thinner or weaker cell walls associated with the higher extent of foaming, lower alumina loading and soapnut amount (Table 2).

Foams produced from (35, 15) and (35, 20) slurries containing higher percentage of soapnut extract were unstable and collapsed during drying at ambient temperature (30 °C) as well as at 40 °C. Apparently, the significantly greater amount of soapnut prolonged the drying time due to the association of water molecules with the carbohydrates in the soapnut extract. Drying at higher temperature solved the above problem resulting in defect free foams. In these samples the presence of higher soapnut amount strengthened the cell walls preventing expansion of cells as experienced in foams from 35 vol% with lower binder amounts.

Drying of foams made from 45 vol% slurries—(45, 2) and (45, 5) showed similar behaviour as that of the (35, 5) and (35, 10) slurries. The foams made from the 45 vol% slurries collapsed when dried at 30 °C and the nature of defect transformed to delamination cracks when drying was carried out at 40 °C due to differential drying effects as explained earlier. Unlike the foams made from 35 vol% slurries, the foams made from 45 vol% slurries, when dried at 50 °C, did not form longitudinal cracks as these foams were more resistant to expansion (Table 2). Foams made from all other slurries, as shown in Table 2, neither collapsed nor cracked at any of the drying temperatures due to lesser amount of water needed to be removed during drying, thicker cell walls due to lower extent of foaming in most cases and inherently stronger cell walls due to higher binder (soapnut amount) as well as ceramic loading.

As discussed above the problems of defects such as cracks or delamination in foams prepared from several of the 35 and 45 vol% slurries could not be solved with changes in drying temperature. Also stable foams could never be made using 35 vol% slurries with 2 wt% soapnut in the premix. An alternative approach was considered for addressing the above difficulties. Since collapse of the foams was attributed to high drainage rate leading to instability of foams [68] before drying could freeze the foam structure, an additive that could reduce the drainage rate was desired. The formation of cracks in foam samples during drying could possibly be minimized with development of cell walls with greater strength. Stronger cell walls could be achieved either by introduction of a more effective binder phase or through enhancement in slurry viscosity which was expected to cause reduction in the extent of foaming and thus thicker cell walls.[69–77]

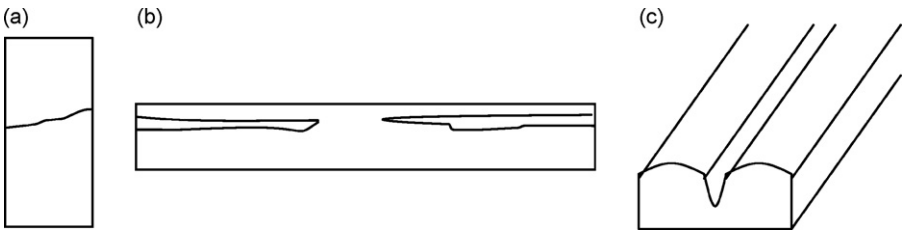

Fig. 3. Schematic of crack patterns observed in some compositions of the dried foam samples (a) top view of a width wise crack accompanying collapse of foams at 30 °C (b) side view of delamination cracks developed during drying at 40 °C and (c) longitudinal crack developed during drying at 50 °C or above due to expansion of bubbles.

Among the natural materials, guar gum a polysaccharide has been commonly used as a foam stabilizer and binder in foods and as a viscosity modifier in other applications.[73–75] Deriving inspiration from these uses of guar gum, it was decided to replace a part of the soapnut in the premix specially for foams made from lower wt% soapnut, which were more susceptible to development of cracks during drying. A comparison of the drainage rate of aqueous foams made from 5 wt% soapnut and soapnut–guar gum mix respectively was carried out by observing the solvent drainage as a function of time. The foams were made under identical conditions by mechanical stirring. It was seen that the presence of 0.5 wt% guar gum reduced the drainage rate from 0.95 ml/s for pure soapnut-based foam to 0.17 ml/s for soapnut–guar gum foams.

As per the expectations, the addition of guar gum enhanced the slurry viscosity significantly.[74,75] The presence of guar gum in the slurries had a dramatic influence on stability of foams prepared from 35 vol% slurries with 2 wt% binder in the premix. From being unstable earlier, highly stable foams that could also be subjected to subsequent processing were prepared. The sintered foam sample prepared from the above slurry composition had 88% porosity with a homogeneous microstructure. For other slurry compositions also, the addition of guar gum eliminated the previously encountered problems of foam collapse, cracking and delamination. All foam samples produced with guar gum addition were free of defects.

3.3. Microstructural evolution in sintered foams

In addition to the defects formed, most of the microstructural changes in the foam structure also took place during the stage of drying. Since the largest number of defect free foam samples were produced by drying at 40 °C (Table 2), the discussion that follows mainly concerns foam samples prepared by drying at 40 °C.

3.3.1. Cell size gradients

It was seen that foam samples, made from some of the slurry compositions developed cell size gradients during drying, though the foamed slurries were nearly homogeneous prior to casting. The gradient in cell size in sintered foam was always such that the cells at the top face which was the only exposed surface during drying had the smallest cells while the bottom-unexposed surface had the largest cells. The gradient in cell size was largest for the composition that had the smallest percentage of soapnut 0.39 wt% with respect to alumina powder weight.

The most severe gradient in cell size was seen for the foam samples made from 55 vol% slurry with 2 wt% soapnut in water which corresponded to 0.39% of soapnut with respect to alumina, the least amount among all compositions (Table 2). Similarly the foams made from 45 vol% slurries with the least soapnut content of 0.6 wt% had the highest cell size gradient. With increase in soapnut content from 0.39 wt% (55, 2) to 0.6 wt% (45, 2) slurry composition, the gradient was less where as it could be expected more because of higher extent of foaming. It is thus likely that the foamed ceramic slurries for a given composition, with soapnut amount lesser than a critical amount experienced coalescence of air bubbles near to the bottom-unexposed surface. The bottom surface is the last to dry providing sufficient time for rearrangements in foam structure.

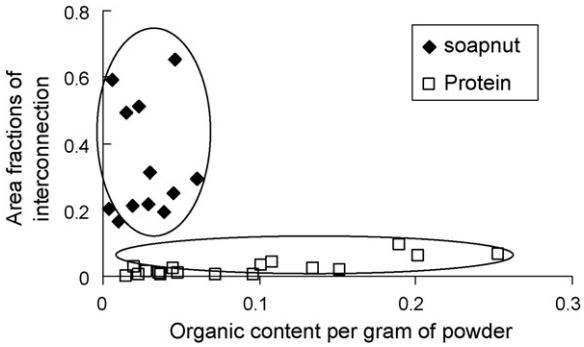

Fig. 4. Fraction area of interconnection of sintered foams produced using both soapnut and protein in alumina slurry.

Lack of soapnut amount in the slurry below a critical amount (example slurry no. 15, Table 1) may not be able to stabilize very fine air bubbles of correspondingly larger air–slurry interface.[71] Coalescence of air bubbles to an extent where sufficient surfactant (soapnut) is available with respect to air–slurry interface may lead to a more stable foam structure.[68] Experiments demonstrated that the presence of higher soapnut amounts appeared to minimize the coalescence of bubbles and thus resulted in smaller gradient in cell size.

3.3.2. Interconnection development

The soapnut-based foams had an exceptionally open structure with larger area of interconnection between the individual cells as [58] compared to foams of similar total porosity produced from other processes like gelcasting or protein coagulation casting (PCC).[50–53] These microstructural differences were quantified in form of a parameter “area fraction of interconnection” which was fraction of the projected area of the interconnections (windows between cells) and the total projected sample area. For foam samples produced from any soapnut-based slurries, the minimum value of area fraction of interconnection was greater than the highest value obtained for foams produced from protein coagulation casting (Fig. 4).

The above differences in microstructure can possibly be understood in terms of the much higher strength of cell walls obtained from binders that undergo gelation as compared to strength of cell walls in soapnut-based foams. During water evaporation the cell walls lose the viscoelastic behaviour,[59] and the air pressure within the individual cells built up which may force the wall to break giving rise to greater number of interconnections between cells. The fact that interconnections between cells for soapnut-based foams do form during the drying stage has been confirmed (Fig. 5). During drying of foam samples constant acoustic emission, though not quantified or measured, was noted which is possibly linked to the above mentioned breakage of the cell walls to open up interconnections.

The differences between the inherent strength of the cell walls in foams produced from different processes could also be interpreted in terms of the flexural strength of the dense green bodies

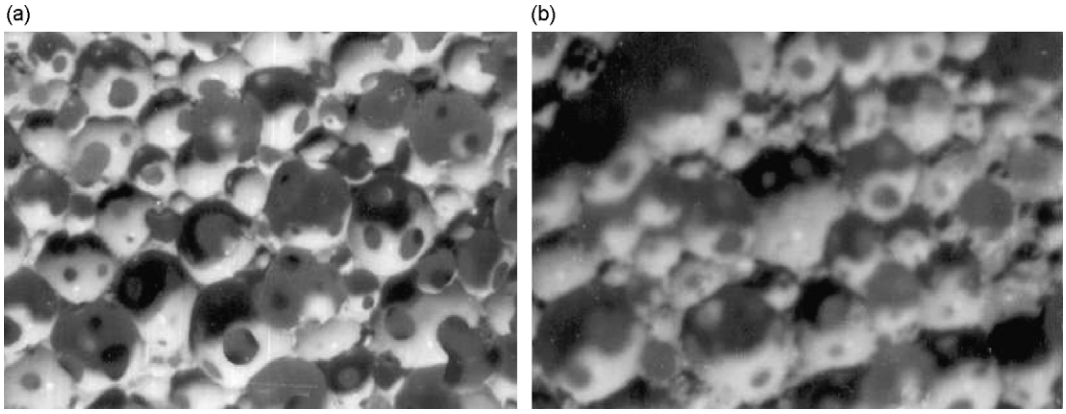

Fig. 5. Stereo-micrographs, at 21×, of alumina foam samples (a) after drying and (b) after binder burn out.

Table 3
Flexural strength of green bars prepared from 55 vol% slurries with different binders in premix (wt%)

Binder	Green flexural strength (MPa)
None	1.1
Soapnut (20 wt%)	2.3
PCC[a] (20 wt% ovalbumin)	4–6
Gelcast (15 wt%)	10
Soapnut + guargum (5 wt%)	1.7
Sucrose (30 wt%)	8.6

[a] 50 vol% alumina slurries.

prepared from different processes including gelcasting, protein coagulation casting and soapnut, respectively (Table 3). It was clearly seen that the gel forming materials resulted in flexural strength that was several factors higher than that of soapnut-based samples.

As mentioned earlier, addition of guar gum resulted in increase in the strength of the foam samples implying an increase in the strength of the cell walls. Thus, foams produced from soapnut–guar gum-based slurries showed lesser connectivity between cells as compared to that in foams prepared from soapnut-based slurries.

3.3.3. Cell size and cell connectivity

The drying temperature had a significant effect on the extent of connectivity between cells as seen from the differences in microstructure of foams dried at 40 °C and 60 °C. The foams produced from 35 vol% slurries when dried at 60 °C showed expansion of cell size from 293 μm to 668 μm, associated with thinning of cell walls and thus number of interconnections per cell increased from 3.4 to 4.1 (Fig. 6). Slurries that foamed to lesser extent and had stronger cell walls due to higher ceramic loading exhibited little expansion of cells (from 266 μm to 299 μm) but did clearly show increase in extent of interconnection from 1.8 to 2.8 when dried at temperature of 60 °C.

The number and area of interconnection between cells in foams was not uniform throughout the sample volume. The connectivity between cells appeared to be higher near the sample surface that was exposed during drying as compared to the bottom-unexposed surface (Fig. 7). This gradient in connectivity between cells from top to bottom surface within the same sample was related to the cell size gradient observed in foams as described earlier in this chapter. In general the cells at the unexposed bottom surface of the foams were larger owing to coalescence and thus had thicker cell walls, which reduced the number of interconnections per cell from 3.9 to 2.9 (Fig. 7). The top surface of the sample dries soon after foamed slurry is cast

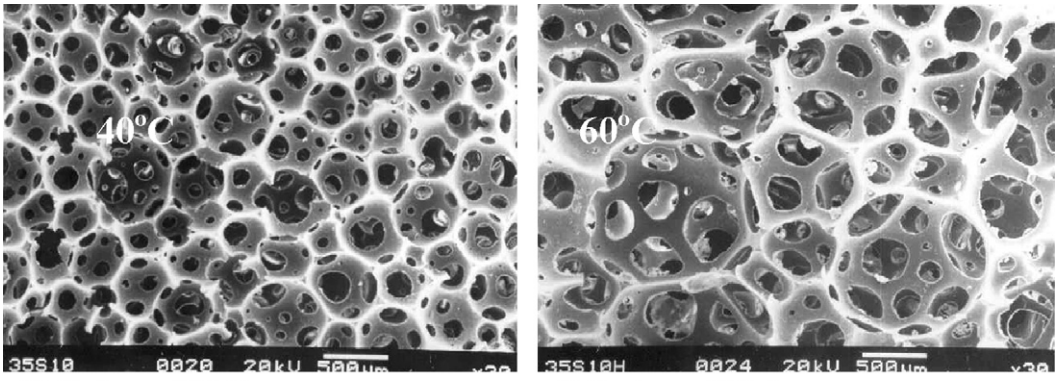

Fig. 6. SEM micrographs depicting change in average cell size and number of windows per cell with drying temperature with 35 vol% alumina loading.

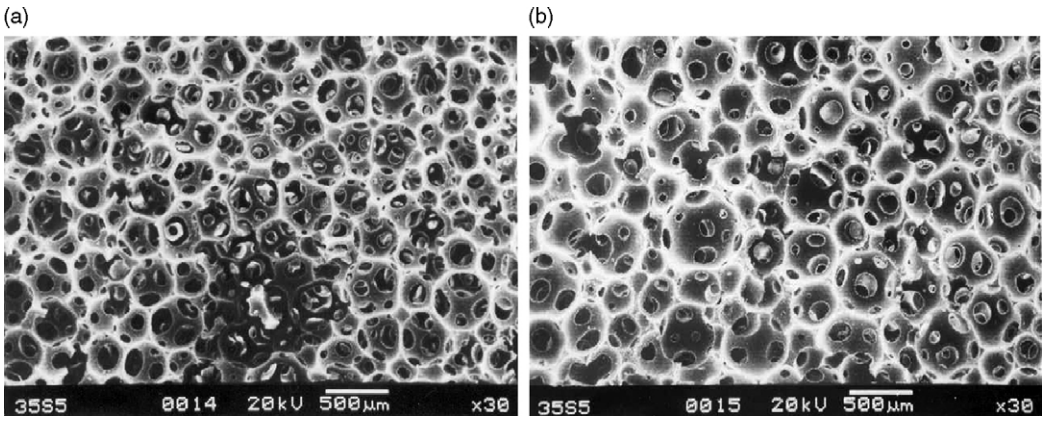

Fig. 7. SEM micrographs of sintered foams from 35 vol% slurries showing interconnection near (a) top and (b) bottom surface.

and thus the cell size was close to that in the foamed slurry. The smaller cells at the top surface had higher air pressure, thinner cell walls and thus exhibited greater connectivity (Fig. 7).

3.4. Binder burn out and sintering of foams

Soapnut components showed decomposition in five stages as seen from the TG (Fig. 8a) as well as the DTG plot (Fig. 8b) that showed five distinct peaks at 150, 210, 330, 430 and 570 °C, respectively. In view of the thermal degradation behaviour of the soapnut, the binder burn out of the green foams was carried out slowly in steps up to 600 °C and then in a single step up to 900 °C with a hold of 1 h. During the gradual heating to 600 °C dwell of half an hour each at temperatures with interval of 30 °C starting from 120 to 300 °C followed by 1 h dwell each at 330, 430 and 570 °was provided. Despite the above slow binder burn out schedule in accordance with soapnut degradation behaviour a large majority of the foam samples appeared to develop cracks during sintering.

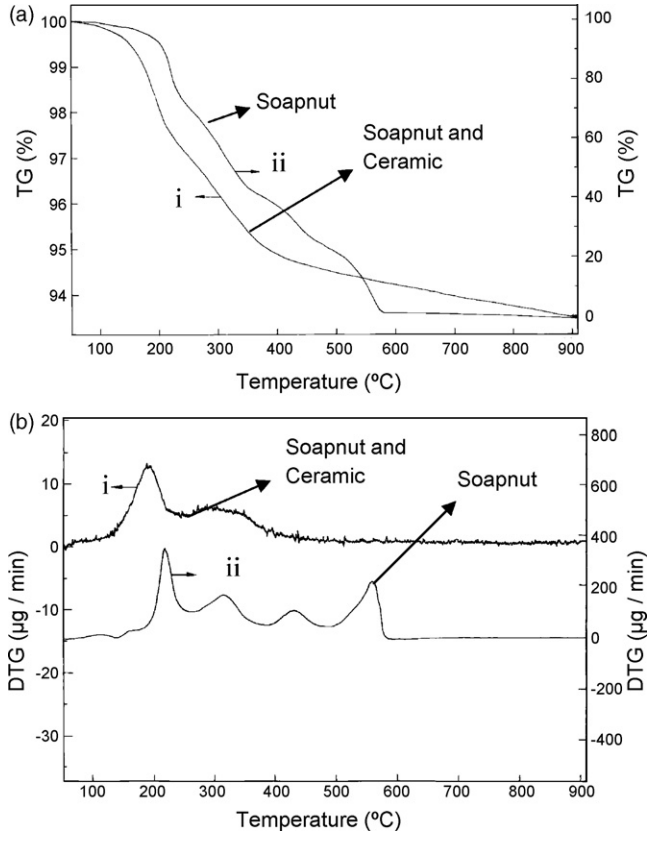

Fig. 8. (a) Thermogravimetric (b) differential thermogravimetric analysis of (i) green alumina foam containing soapnut and (ii) soapnut.

A comparison of the TG analysis of the green ceramic foam with that of pure soapnut revealed the reason for the above cracking. Association of the soapnut components with the ceramic powder particles possibly resulted in a single stage gradual weight loss at higher temperatures that started from around 380 °C and continued up to nearly 900 °C. This continued weight loss upto 900 °C for soapnut-based green ceramic foam samples was in contrast with the behaviour of pure soapnut, which showed complete burnout by about 580 °C. As a result of the above analysis when the foam samples were subjected to binder burn out with continued slow heating between 600 and 900 °C crack-free samples were obtained after sintering.

4. Summary and conclusions

The reproducibility of soapnut extract in terms of composition and concentration was checked using UV–vis spectroscopy and used successfully to make ceramic foams in varying range of porosities. Soapnut served multiple functions including that of foaming agent, binder and stabilizer. The setting of soapnut-based foams could be achieved simply by drying without requiring any gelation step. Removal of soapnut from the dried foamed body requires slow heating. The defects developed during consolidation of foamed slurry were addressed by controlling drying temperature and with partial replacement of soapnut amount with guar gum especially for the samples made from lower soapnut amount. Microstructural inhomogenities such as cell size gradient through out the thickness of foamed samples, were eliminated by using higher concentration of soapnut. The extent of cell connectivity was high and unique in comparison to other direct casting and foaming processes. The high cell connectivity was related to the poor strength of the cell wall, which ruptures during drying.

Acknowledgements

Authors are thankful to CSIR, New Delhi under scheme no. 03 (0917)/00-EMR-II and 9/81 (492)/04-EMR-I for financial support and R.T. Vanderbilt for providing Darvan 821A sample for research purposes. We are also grateful to Dr. Santanu Dhara for providing data on protein coagulation-based ceramic foams.

References

1. Gibson, L. J. and Ashby, M. F., *Cellular Solids: Structure, and Properties*. Pergamon Press, Oxford, UK, 1988.
2. Schwartzwalder, K. and Somers, A.V., Method of making porous ceramic particles. U.S. Patent No. 3,090,094, 21 May 1963.
3. Matthews, S. and Pickrell, G., A new generation of low-mass kiln furniture. *Am. Ceram. Soc. Bull.*, 1999, 77–78.
4. Trimis, D. and Drust, F., Combustion in a porous medium-advances and applications. *Combust. Sci. Technol.*, 1996, **121**, 153–168.
5. Karus, M., Eliasson, B., Kogelschatz, U. and Wokaun, A., CO_2 reforming of methane by the combination of di-electric barrier discharges and catalysis. *Phys. Chem. Chem. Phys.*, 2001, **3**, 294–300.
6. Minh, N. Q. and Takahashi, T., *Science and Technology of Ceramic Fuel Cells*. Elsevier Science, 1995.
7. Kang, I., Kim, T., Ko, K., Song, H., Goto, T. and Lee, B., Microstructure and osteoblast adhesion of continuously porous Al_2O_3 body fabricated by fibrous monolithic process. *Mater. Lett.*, 2005, **59**, 69–73.
8. Haugen, H., Will, J., Kohler, A., Hopfner, U., Aigner, J. and Wintermantel, E., Ceramic TiO_2-foams: characterisation of a potential scaffold. *J. Eur. Ceram. Soc.*, 2004, **24**, 661–668.
9. Koc, N., Timucin, M. and Korkusuz, F., Fabrication and characterization of porous tricalcium phosphate ceramics. *Ceram. Int.*, 2004, **30**, 205–211.
10. Lin, K., Chang, J., Zeng, Y. and Qian, W., Preparation of macroporous calcium silicate ceramics. *Mater. Lett.*, 2004, **58**, 2109–2113.
11. Zhu, X., Jiang, D. and Tan, S., Preparation of silicon carbide reticulated porous ceramics. *Mater. Sci. Eng. A*, 2002, **323**, 232–238.
12. Atisivan, R., Bose, S. and Bandyopadhyay, A., Porous mullite preforms via fused deposition. *J. Am. Ceram. Soc.*, 2001, **84**(1), 221–223.
13. Ota, T., Takahashi, M., Hibi, T., Ozawa, M., Suzuki, S. and Hikichi, Y., Biomimetic process for producing SiC "wood". *J. Am. Ceram. Soc.*, 1995, **78**(12), 3409–3411.
14. Qian, J., Wang, J., Qiao, G. and Zin, Z., Preparation of porous SiC ceramic with a wood like microstructure by sol–gel and carbothermal reduction processing. *J. Eur. Ceram. Soc.*, 2004, **24**, 3251–3259.
15. Vogli, E., Seiber, H. and Greil, P., Biomorphic SiC–ceramic prepared by Si-vapor phase infiltration of wood. *J. Eur. Ceram. Soc.*, 2002, **24**, 2663–2668.
16. Greil, P., Biomorphous ceramics from lignocellulosics. *J. Eur. Ceram. Soc.*, 2001, **21**, 105–118.
17. Qian, J., Jin, Z. and Wang, X., Porous SiC ceramics fabricated by reactive infiltration of gaseous silicon into charcoal. *Ceram. Int.*, 2004, **30**, 947–951.
18. Vogli, E., Mukerji, J., Hoffman, C., Kaldny, R., Seiber, H. and Greil, P., Conversion of oak to cellular silicon carbide ceramic by gas-phase reaction with silicon monoxide. *J. Am. Ceram. Soc.*, 2000, **84**(6), 1236–1240.
19. Zollfrank, C., Kladny, R., Seiber, H. and Greil, P., Biomorphous SiOC/C–ceramic composites from chemically modified wood templates. *J. Eur. Ceram. Soc.*, 2004, **24**, 479–487.
20. Zollfrank, C. and Seiber, H., Microstructure and phase morphology of wood derived biomorphous Si SiC–ceramics. *J. Eur. Ceram. Soc.*, 2004, **24**, 495–506.
21. Streitwieser, D. A., Popovska, N., Gerhard, H. and Emig, G., Processing of biomorphous SiC ceramics from paper preforms by chemical vapor infiltration and reaction (CVI–R) technique. *Ceram. Eng. Proc.*, 2004, **25**(3), 511–516.
22. Qian, J., Wang, J., Jin, Z. and Qiao, G., Preparation of macroporous SiC from Si and wood powder using infiltration-reaction process. *Mater. Sci. Eng. A.*, 2003, **358**, 304–309.
23. Ota, T., Imaeda, M., Takase, H., Kobayashi, M., Kinoshita, N., Hirashita, T., Miyazaki, H. and Hikichi, Y., Porous titania ceramic prepared by mimicking silicified wood. *J. Am. Ceram. Soc.*, 2000, **83**(6), 1521–1523.
24. Popovska, N., Streitwieser, D. A., Xu, C. and Gerhard, H., Processing of porous biomorphic TiC ceramics by chemical vapor infiltration and reaction (CVI–R) technique. *Ceram. Eng. Proc.*, 2004, **25**(3), 535–540.
25. Popovska, N., Streitwieser, D. A., Xu, C. and Gerhard, H., Paper derived biomorphic porous titanium carbide and titanium oxide ceramics produced by chemical vapor infiltration and reaction (CVI–R). *J. Eur. Ceram. Soc.*, 2005, **25**, 829–836.
26. Miao, X., Hu, Y., Liu, J. and Wong, A. P., Porous calcium phosphate ceramics prepared by coating polyurethane foams with calcium phosphate cements. *Mater. Lett.*, 2004, **58**, 397–402.
27. Roncari, E., Galassi, C. and Bassarello, C., Mullite suspensions for reticulate ceramic preparation. *J. Am. Ceram. Soc.*, 2000, **83**(12), 2993–2998.
28. Tulliani, J., Montanaro, L., Bell, T. J. and Swain, M. V., Semiclosed-cell mullite foams: preparation and macro- and micromechanical characterization. *J. Am. Ceram. Soc.*, 1999, **82**(4), 961–968.
29. Zhu, X., Jiang, D. and Tan, S., Improvement in the strength of reticulated porous ceramics by vacuum degassing. *Mater. Lett.*, 2001, **51**, 363–367.
30. Zhu, X., Jiang, D. and Tan, S., The control of slurry rheology in the processing of reticulated porous ceramics. *Mater. Res. Bull.*, 2002, **37**, 541–553.
31. Zhu, X., Jiang, D., Tan, S. and Zhang, Z., Improvement in the strut thickness of reticulated porous ceramics. *J. Am. Ceram. Soc.*, 2001, **84**(7), 1654–1656.
32. Pu, X., Liu, X., Qiu, F. and Huang, L., Novel method to optimize the structure of reticulated porous ceramics. *J. Am. Ceram. Soc.*, 2004, **87**(7), 1392–1394.
33. Cichocki, F. R. and Trumble Jr., K. P., Tailored porosity gradients via colloidal infiltration of compression-molded sponges. *J. Am. Ceram. Soc.*, 1998, **81**(6), 1661–1664.
34. Lyckfeldt, O. and Ferreira, J. M. F., Processing of porous ceramics by starch consolidation. *J. Eur. Ceram. Soc.*, 1998, **18**, 131–140.
35. Li, S., Wijn, J., Layrolle, P. and Groot, K., Novel method to manufacture porous hydroxyapatite by dual-phase mixing. *J. Am. Ceram. Soc.*, 2003, **86**(1), 65–72.
36. Diaz, A. and Hampshire, S., Characterisation of porous silicon nitride materials produced with starch. *J. Eur. Ceram. Soc.*, 2004, **24**, 413–419.
37. Tang, F., Fudouzi, H. and Sakka, Y., Fabrication of macroporous alumina with tailored porosity. *J. Am. Ceram. Soc.*, 2003, **86**(12), 2050–2054.
38. Thijs, I., Luyten, J. and Mullens, Steven, Producing ceramic foams with hollow spheres. *J. Am. Ceram. Soc.*, 2003, **87**(1), 170–172.
39. Maca, K., Dobsak, P. and Boccaccini, A. R., Fabrication of graded porous ceramics using alumina–carbon powder mixtures. *Ceram. Int.*, 2001, **27**, 577–584.
40. Colombo, P., Bernardo, E. and Biasetto, L., Novel microcellular ceramics from a silicone resin. *J. Am. Ceram. Soc.*, 2004, **87**(1), 152–154.
41. Colombo, P., Gambaryan-Roisman, T., Scheffler, M., Buhler, P. and Greil, P., Conductive ceramic foams from preceramic polymers. *J. Am. Ceram. Soc.*, 2001, **84**(10), 2265–2268.
42. Schmidt, H., Koch, D., Grathwohl, G. and Colombo, P., Micro-/macroporous ceramics from preceramic precursors. *J. Am. Ceram. Soc.*, 2001, **84**(10), 2252–2255.
43. Kim, S. H., Kim, Y. W. and Park, C. B., Effect of inert filler addition on pore size and porosity of closed-cell silicon oxycarbide foams. *J. Mater. Sci.*, 2004, **39**, 3513–3515.
44. Peng, H. X., Fan, Z, Evans, J. R. G. and Busfield, J. J. C., Microstructure of ceramic foams. *J. Eur. Ceram. Soc.*, 2000, **20**(7), 807–813.
45. Nangrejo, M. R., Bao, X. and Edirisinghe, M. J., Preparation of silicon carbide–silicon nitride composite foams from pre-ceramic polymers. *J. Eur. Ceram. Soc.*, 2000, **20**, 1777–1785.
46. Powell, S. J. and Evans, J. R. G., The Structure of ceramic foams prepared from polyurethane–ceramic suspensions. *Mater. Manuf. Process.*, 1995, **10**(4), 757–771.
47. Peng, H. X., Fan, Z. and Evans, J. R. G., Factors affecting the microstructure of a fine ceramic foam. *Ceram. Int.*, 2000, **26**, 887–895.
48. Zhang, W., Wang, H. and Jin, Z., Gelcasting and properties of porous silicon carbide/silicon nitride composite ceramics. *Mater. Lett.*, 2005, **59**, 250–256.

49. Katsuki, H., Kawahara, A. and Ichinose, H., Preparation and some properties of porous alumina ceramics obtained by the gelatination of ammonium alginate. *J. Mater. Sci.*, 1992, **27**, 6067–6070.
50. Innocentini, M. D. M., Sepulveda, P., Salvini, V. R., Pandolfeli, V. C. and Coury, J. R., Permeability and structure of cellular ceramics: a comparison between two preparation techniques. *J. Am. Ceram. Soc.*, 1998, **83**(12), 3349–3352.
51. Binner, J. G. P., Production and properties of low density engineering ceramic foams. *Brit. Ceram. Trans.*, 1997, **96**(6), 247–249.
52. Dhara, S. and Bhargava, P., A simple direct casting route to ceramic foams. *J. Am. Ceram. Soc.*, 2003, **86**(10), 1645–1650.
53. Dhara, S., Rheology of aqueous alumina slurries and their use in gelation forming of dense and porous alumina shapes and structures. Ph.D. Thesis, IIT, Kharagpur, 2003.
54. Studart, A. R., Gonzenbach, U. T., Tervoort, E. and Gauckler, L. J., Processing routes to macroporous ceramics: a review. *J. Am. Ceram. Soc.*, 2006, **89**(6), 1771–1789.
55. Pradhan, M. and Bhargava, P., Effect of sucrose on fabrication of ceramic foams from aqueous slurries. *J. Am. Ceram. Soc.*, 2005, **88**(1), 216–218.
56. Pradhan, M., Processing and microstructure of alumina foams produced by direct foaming of sucrose and soapnut based aqueous alumina slurries. Ph.D. Thesis, IIT, Kharagpur, 2006.
57. Pradhan, M. and Bhargava, P., A simple environment friendly process for fabrication of highly porous materials. Indian Patent 473/KOL/2003.
58. Dhara, S., Pradhan, M., Ghosh, D. and Bhargava, P., Nature inspired novel processing routes for ceramic foams. *Adv. Appl. Ceram.*, 2005, **104**, 1–13.
59. Holmes, D. M., Kumar, R. V. and Clegg, W. J., Cracking during lateral drying of alumina suspensions. *J. Am. Ceram. Soc.*, 2006, **89**(6), 1908–1913.
60. Lan, W. and Xiao, P., Constrained drying of aqueous yttria-stabilized zirconia slurry on a substrate. I. Drying mechanism. *J. Am. Ceram. Soc.*, 2006, **89**(5), 1518–1522.
61. Dubois, M., Gilles, K. A., Hamiltonian, J. K., Rebers, P. A. and Smith, F., Colorimetric method for determination of sugars and related substances. *Anal. Chem.*, 1956, **28**(3), 350–356.
62. Nagornaya, V. A., Zhizhina, R. G. and Kartashov, A. K., Determination of saponin in the products of sugar production. *Sakharnaya promyshlennost*, 1966, **40**(8), 39–44 (Russian Journal) (1946–1987).
63. Sarin, J. L. and Beri, M. L., Extraction of saponin from soapnut. *Ind. Eng. Chem.*, 1939, **31**(6), 712–713.
64. Row, L. R. and Rukmini, C., Chemistry of saponins. Part I. Saponin of *Sapindus mukorossi* garten. *Indian J. Chem.*, 1966, **4**, 36–38.
65. Pathak, D. N. and Pant, G. N., Influence of soapnut on capillarity control. *J. Indian Chem. Soc.*, 1975, 691–694.
66. Nomura, O., Nakamura, R. and Hotta, S., Carbon-containing refractory and its manufacture using carbohydrate binder, Shinagawa Refractories Co. Ltd., Japan, 1998, JP 97-14382 19970128.
67. Ortega, F. S., Sepulveda, P., Innocentini, M. D. M. and Pandolfeli, V. C., Surfactants. *Am. Ceram. Soc. Bull.*, 2001, **80**(4), 37–42.
68. Sebba, F., *Foams and Biliquid foams-Aphrons*. John Wiley and Sons, New York, 1987, pp. 22–23.
69. Langevin, D., Surface energy and surface rheology relation to foam properties. Foams and Emulsions. In *NATO ASI Series*, *354*, ed. J. F. Sadoc and N. Rivier. Kluwer Academic Publishers, 1999, pp. 1–10.
70. Gaines, G., *Insoluble monolayers at liquid–gas interfaces*. Wiley, New York, 1966;
    Exerowa, D., Kashchiev, D. and Platikanov, D., *Adv. Colloid Interf. Sci.*, 1992, **40**, 201.
71. Garrett, P. R., In *Defoaming: Theory and Industrial Applications*, ed. P. R. Garrett. Marcel Dekker, New York, 1993.
72. Aveyard, R., Binks, B. P., Clint, J. H. and Fletcher, P. D. I., Foams and emulsions: their stability and breakdown by solid particles and liquid droplets. In *NATO ASI Series*, *354*, ed. J. F. Sadoc and N. Rivier. Kluwer Academic Publishers, 1999, pp. 1–10.
73. Rosen, M. J., *Surfactants and Interfacial Phenomena*. John Wiley and Sons, New York, 1989, pp.277–303.
74. Sarma, D. S. H., Pandit, J. and Khilar, K. C., Enhancement of stability of aqueous foams by addition of water-soluble polymers—measurements and analysis. *J. Colloid Interf. Sci*, 1988, **124**(1), 339–348.
75. Pradhan, M. S., Sarma, D. S. H. and Khilar, K. C., Stability of aqueous foams with polymer additives. II. Effects of temperature. *J. Colloid Interf. Sci.*, 1990, **139**(2), 519–526.
76. Foams: theory, measurements and applications. In *Surfactant Science Series,*, *57*, ed. R. K. Prud'hommer and S. A. Khan. Marcel Dekker, 1996.
77. Pugh, R. J., Foaming, foam films, antifoaming and defoaming. *Adv. Colloid Interf. Sci.*, 1996, **64**, 167-142.